Journal of Computer Assisted Tomography
8(3):429–436, June

Direct Cardiac NMR Imaging of Heart Wall and Blood Flow Velocity

P. van Dijk

Abstract: Nuclear magnetic resonance (NMR) imaging is used to produce in the same scan both anatomical and functional information of the heart and great vessels. A method is described to generate velocity images by the use of phase shifts for moving spins induced by imaging gradients under electrocardiogram (ECG) synchronized imaging conditions. The influence of the different gradients is discussed together with methods to obtain velocity information for each gradient direction separately. The results, obtained with a 0.14 T resistive NMR scanner and normal volunteers, show the spatial velocity distribution in the aorta and heart walls in color scale images. The feasibility of velocity calculations is demonstrated and some applications are given. The present results indicate the possibility of quantitative flow and motion analysis with ECG synchronized NMR imaging. **Index Terms:** Nuclear magnetic resonance—Nuclear magnetic resonance, techniques—Heart—Heart, blood flow—Gating, ECG.

The noninvasive character of nuclear magnetic resonance (NMR) imaging and the absence of obscuration by bone structures make it a desirable technique for heart imaging. The relative long scan times needed, however, give rise to motion artifacts. Synchronization of the imaging sequences to the heart cycle can greatly reduce these artifacts (1). The capability of imaging in any phase of the cardiac cycle makes it possible to use NMR for volumetric measurements from end-systole and end-diastole images. Also, the evaluation of motion is possible by displaying images from consecutive phases in a movie loop. Several authors have reported on the use and benefits of NMR imaging for displaying the anatomy of the heart and great vessels, both untriggered (2) and electrocardiogram (ECG)-triggered (3–5). Apart from showing fine anatomical details in the heart, NMR heart imaging holds promise for tissue characterization as well, important for the detection and sizing of infarcts (6–9). Using velocity images, heart wall motion and blood flow speeds can also be quantitated with NMR imaging. This report deals with some methods to obtain this functional information with the same gradients used for anatomical imaging. Other methods have previously been reported in the literature (10).

Address correspondence and reprint requests to Dr. van Dijk at Philips Medical Systems, NMR Science, geb. HOI, Veenpluis 2, 5684 PC Best, The Netherlands.

MATERIALS AND METHODS

In the two-dimensional Fourier transform (2DFT) imaging method that we use, the NMR image is reconstructed from time signals by a complex 2DFT. For a 128 × 128 pixel image matrix, the signals are obtained in 128 consecutive imaging sequences. For heart imaging each sequence is triggered by a pulse derived from the R-wave of the patient's ECG (Fig. 1). The delay of this pulse determines the imaging phase in the cardiac cycle. Each sequence consists of a series of radiofrequency (RF) and magnetic field gradient pulses, respectively, for evoking a signal and providing spatial information in the signal. A gradient magnetic field applied after an RF excitation pulse (90° pulse) makes the spins at different locations in the excited slice precess at different frequencies. The spins start to dephase with respect to the resonant frequency phase (11). For a given location the associated phase shift is proportional to the gradient amplitude and the time it is active. There is, however, a difference in phase shift for stationary spins and moving spins. For spins moving uniformly in the direction of the gradient, an extra term is added that

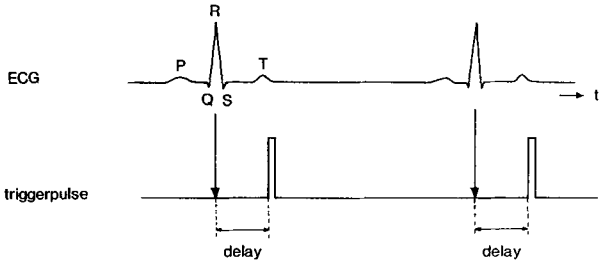

FIG. 1. Illustration of trigger pulse derived from the R-wave pulse of the patient's electrocardiogram (ECG). An adjustable delay determines the imaging phase in the heart cycle. (Reproduced with permission from S. Karger AG, Basel, ref. 1.)

is directly proportional to the velocity in the gradient direction (Fig. 2).

For stationary spins ($x = x_0$) the phase shift at $t = t_2$ is

$$\phi_s = \gamma G_x x_0 (t_2 - t_1) \quad (1)$$

whereas for moving spins ($x = x_0 + v_x \cdot t$) it will be

$$\phi_m = \gamma G_x x_0 (t_2 - t_1) + 1/2 \gamma G_x v_x (t_2^2 - t_1^2) \quad (2)$$

Where γ is the gyromagnetic ratio, G_x is the gradient magnetic field in X-direction, x_0 is the x-coordinate of spins at the moment of excitation (90° RF pulse) and v_x is the velocity of spins in X-direction.

In most imaging methods spin echo sequences are used for the purpose of reducing the influence of field inhomogeneities, which also cause dephasing and unwanted signal decay. A 180° pulse is applied, which forms an echo by rephasing of the spins. This echo signal is measured in the presence of a measuring gradient, in our example for instance G_x.

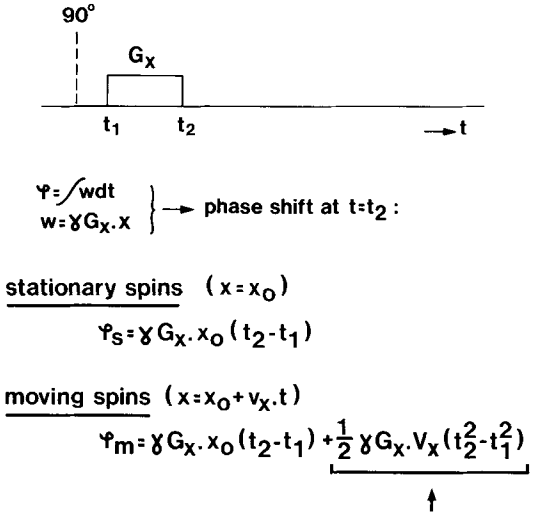

FIG. 2. Effect of a gradient (G_x) on the phase of stationary and moving spins. For moving spins an extra term is added that is proportional to the speed in the direction of the gradient (V_x, see arrow).

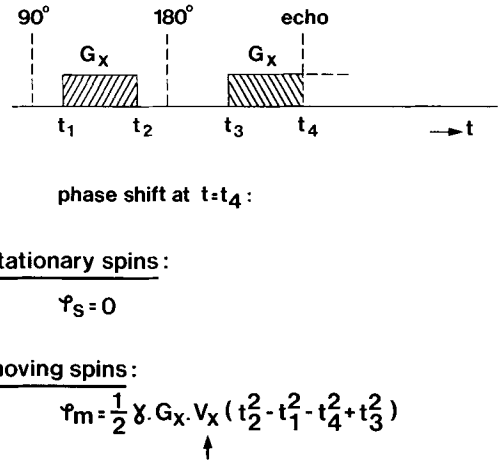

FIG. 3. Effect of a gradient (G_x) on the phase of stationary and moving spins during a spin echo sequence. If the hatched areas per gradient are equal, the net phase shift for stationary and moving spins will be zero, respectively, proportional to V_x at the moment of echo.

Figure 3 shows the situation for a spin echo sequence where the same gradient after the 180° pulse produces a negative phase shift. If the hatched areas are made equal, then for stationary spins the net phase shift at the moment of echo will be zero, which is the desired imaging situation. For moving spins, however, a nonzero net phase shift results, still proportional to v_x.

For stationary spins the phase shift at $t = t_4$ is

$$\phi_s = 0 \quad (3)$$

and for moving spins results

$$\phi_m = 1/2 \gamma G_x v_x (t_2^2 - t_1^2 - t_4^2 + t_3^2) \quad (4)$$

It is this extra phase shift that makes it possible to produce velocity images. For a fixed gradient polarity the sign of this phase indicates the direction

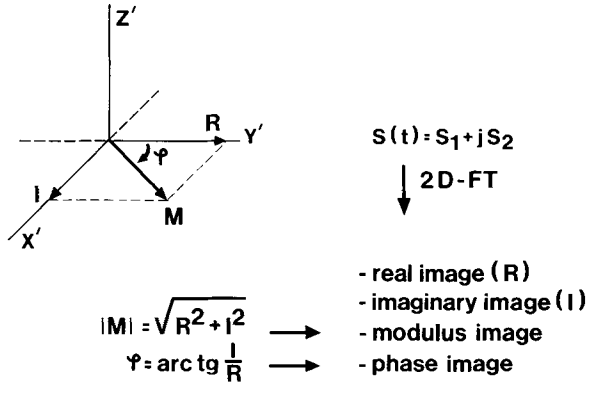

FIG. 4. Illustration of phase-shifted magnetization vector in the rotating frame. From the quadrature phase detected time signals S_1 and S_2, a real and imaginary image can be reconstructed. A modulus and phase image can be calculated from the resulting image data.

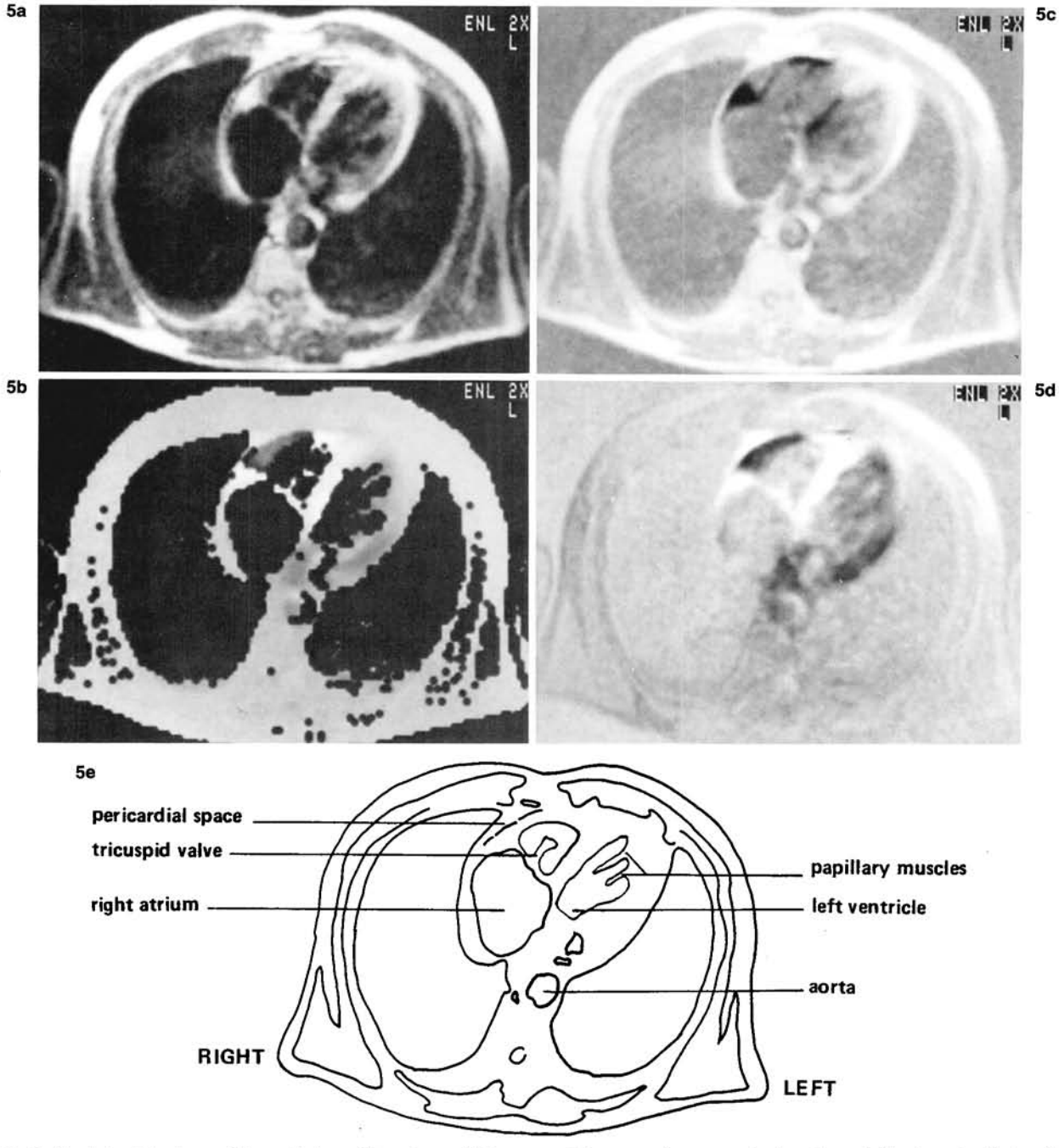

FIG. 5. Modulus **(a)**, phase **(b)**, real **(c)**, and imaginary **(d)** images of the same transversal slice through the heart, obtained in one 8 min scan. Some anatomical details of this slice are indicated in **(e)**.

of motion along the gradient axis, e.g., the X-axis.

To see how phase shifts work out in the NMR image, I discuss briefly the method of detection and image reconstruction. The phase information can be retrieved from the measured signals by using phase sensitive detection or quadrature detection where RF signals are mixed with two reference signals. The result is two low frequency output signals having a 90° phase difference, referred to here as the real and imaginary signals S_1 and S_2. These signals deliver, via a complex 2DFT, the real and imaginary images. From this image data, a modulus and phase image can be calculated also (Fig. 4). The imaging gradients position encode both the real and imaginary signals and hence also the modulus and phase information. With properly tuned gradients (i.e., equal gradient-time integrals on both sides of the 180° pulse), the phase ϕ is zero and the imaginary image will be empty (contain only noise). In case of motion, both the real and imaginary images

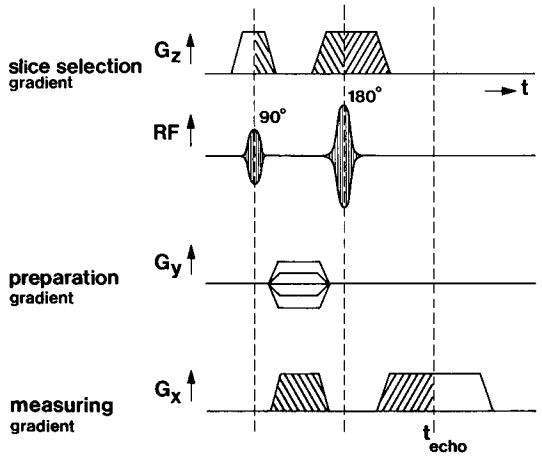

FIG. 6. A practical set of radiofrequency (RF) and gradient waveforms as used for 2DFT imaging. Hatched areas are equal per gradient to give zero phase shifts for stationary spins.

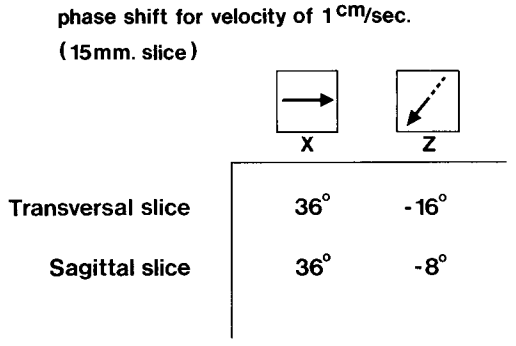

FIG. 7. Calculated phase shifts for spins moving in X- or Z-direction with a speed of 1 cm/s for two imaging plane orientations.

are meaningful. Figure 5 shows all four types of images; Figs. 5a and b are modulus and phase images, respectively, and Figs. 5c and d are real and imaginary images, respectively. Information for all images is obtained in one ECG triggered scan of a 15 mm transversal slice, 180 ms after the R-wave. Anatomical details are shown in Fig. 5e. Black regions in a gray scale real image indicate regions in which the real part of the signal is negative, whereas zero signal is represented in gray as outside the body. In the imaginary image, Fig. 5d, only the regions with moving spins show different intensities since the phase shift for stationary spins is carefully made zero.

In the real and imaginary images gray level is still a function of spin density *and* motion. This is not the case for the phase image, where only phase, and thus velocity, information is depicted. It is important to note that, because of synchronization to the heart cycle, spins in tissue or blood to a great extent show the same velocity during each imaging sequence. This will give the same phase shifts per pixel due to motion in every imaging sequence using the same gradients. After complex 2DFT, the modulus and phase images represent the values at the moment of echo. In the sequences used here, the time between excitation and echo is 50 ms. In the case of nonuniform motion, a velocity average over the active periods of the gradients during this echo time will be imaged.

A practical set of RF and gradient pulses for 2DFT imaging of a transversal slice is shown in Fig. 6. G_z is the slice selection gradient, G_x is the measuring gradient, and G_y is the preparation gradient used for spatial encoding in X- and Y-direction, respectively. The hatched areas are equal per gradient, giving zero phase shift for stationary spins. G_x and G_z have the same amplitudes for all imaging sequences during the scan. Also v_x and v_z will be the same for each sequence due to the motion synchronization, and this leads to constant phase shifts for spins moving in X- or Z-direction. Motion in X-direction also gives rise to a frequency sweep during data acquisition, but in practice this is small compared with the bandwidth per pixel and not noticeable in the image. Motion in Y-direction changes the Y-coordinate of spins in the image, as can be appreciated by rewriting Eq. 2 for this case:

$$\phi_m = \gamma G_y[y_o + v_y \cdot (t_2 + t_1)/2](t_2 - t_1) \quad (5)$$

The difference with stationary spins is the displacement $\Delta y = v_y \cdot (t_2 + t_1)/2$, which is constant for the same v_y, t_1, and t_2 in each sequence. In practice Δy is in the order of the pixel size and negligible in the image. Therefore, motion in Y-direction does not show up in the phase or velocity image. In images shown here the combined effect of motion in two directions, i.e., the slice selection and measuring gradient direction, is present.

Since the velocity per direction is not known, one velocity image would not be enough to quantify the velocity per direction. (Motion in one known direction, however, can be quantified; for example, in a slice perpendicular to the aorta, flow rates in the aorta can be calculated from the phase shift.) One possible solution to the problem is alternating polarity slice selection gradients and measuring and adding two signals for one preparation gradient value, which cancels the equal but opposite sign motion induced phase shifts for this direction. Another possibility is to compensate for the nonzero gradient-time integral for moving spins by adjustment of the slice selection gradient waveform. (Unlike the first method this is only good for one slice thickness determined by the gradient strength.) Each method leaves the measuring gradient as the only motion sensitizing gradient and the phase image will represent only velocities in one direction, obtained in only one scan. Doing the same with interchanged measuring and preparation gradients, an image of velocities in the original prep-

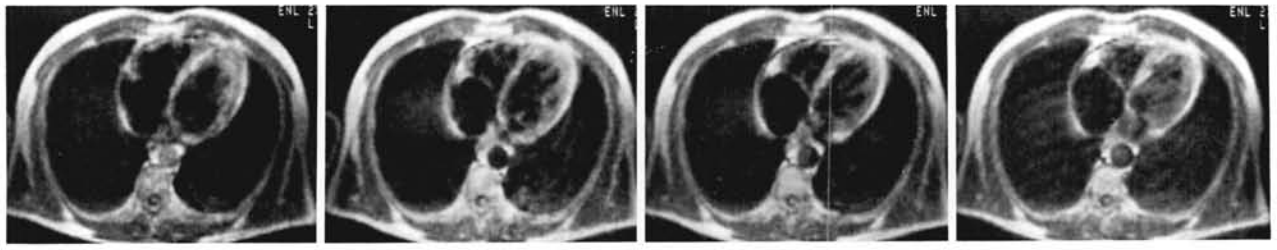

FIG. 8. Modulus images from four transversal scans through the heart in systole at 60 ms intervals. (Reproduced with permission from S. Karger AG, Basel, ref. 1.)

aration gradient direction only can be made. An image of motion perpendicular to the plane can be calculated from two measurements, e.g., one with alternating and one with nonalternating slice selection gradients. In all these cases ECG triggered imaging is assumed. Without this the velocity information cannot be obtained in a single scan due to different velocities in each imaging sequence.

Calculation of the gradient-time integrals for the contributing gradients in transversal and sagittal plane orientations yields figures for phase shifts at 1 cm/s velocity, as shown in Fig. 7. The difference in the second column is caused by differing adjustment gradients. The phases for the image are calculated modulus 360°. In the case of motion in the measuring gradient direction this will give the same value for 1 cm/s (36°) and 11 cm/s (36° + 360°). As this cannot occur for the same pixel, these speeds can be discriminated by counting the number of scales from the zero phase on (stationary spins). A color display of the phase images with a cyclic color scale is found to be useful for this purpose.

RESULTS

All images were made with a Philips resistive NMR scanner with a field strength of 0.14 T, giving a resonance frequency of 6 MHz, and a slice thickness of 15 mm. An image matrix of 128 × 128 pixels is measured; each scan took approximately 8 min using four averages. All velocity information is obtained in the normal imaging process. Figure 8 shows a series of four modulus images of a transversal slice at 60 ms intervals in the cardiac cycle (contraction part). The contraction of the left ventricle, the torsion movement of the heart, the lengthening of papillary muscles, and flow variation in the aorta can be clearly seen. From the same scans, phase images can be calculated that show the velocity per pixel of tissue and slow flowing blood (Fig. 9). Velocity is represented in a cyclic color scale and each of the four scales extends from −180 to +180° upward. Zero phase is represented by green, the color for the stationary anatomy. Other colors indicate motion. Different colors correspond to different velocities. In black areas the phase is not calculated since the real and imaginary pixel values fall below a certain noise threshold. The absence of signal in these areas in the heart is caused by rapid blood flow (12), which also accounts for the natural contrast between blood and heart wall tissue. Figure 10 is again the first one of the series and it represents the early systole situation. The yellow to green transition on the right is caused by a minor misadjustment of the gradients. Flow in the aorta, perpendicular to the plane of imaging, i.e., in only one gradient direction, can be quantitated, thanks to the synchronized imaging sequences. The blue area in the aorta has a measured phase of −96°, meaning a blood flow velocity of 6 cm/s and the violet area was found to have a flow speed of approximately 10 cm/s. The standard deviation in the phase is 5°, giving a statistical error in the flow speed of 0.3 cm/s for this direction.

An interesting application of the velocity image is demonstrated, i.e., the discrimination between heart tissue and slow flowing blood. In modulus images, such as the first scan in Fig. 8, taken at the start of contraction, the right ventricle wall is seemingly thicker than would be expected from the diastolic volume. This is caused by signal from slow flowing or turbulent blood near the inner wall. The velocity image, but also the real and imaginary images, makes this apparent. Thus, for a good determination of left ventricle volume in diastole, this type of image will be very helpful.

Figure 11 is the third velocity image of the series. The measuring gradient is from left to right in the image. Motion in this direction will give a positive shift of 36° per cm/s. From Fig. 8 it can be judged that the blue part of the right atrium is moving to the right in the image. Assuming this part to move purely in X-direction, the tissue velocity can be quantitated as follows. Phase shifts exceeding 180° are displayed by a color from the other end of the cyclic scale, in this case from green through yellow, white, red to blue. The velocity of the blue part is thus approximately 7.5 cm/s. The velocity difference between the slow moving yellow and fast moving blue tissue is made possible by sliding motion of the wall in the heart sac formed by the pericardium. The papillary muscles extend during contraction to the left in the image, which accounts for the negative phase shift and the blue color. The direction of motion can be found from the first color after green.

9

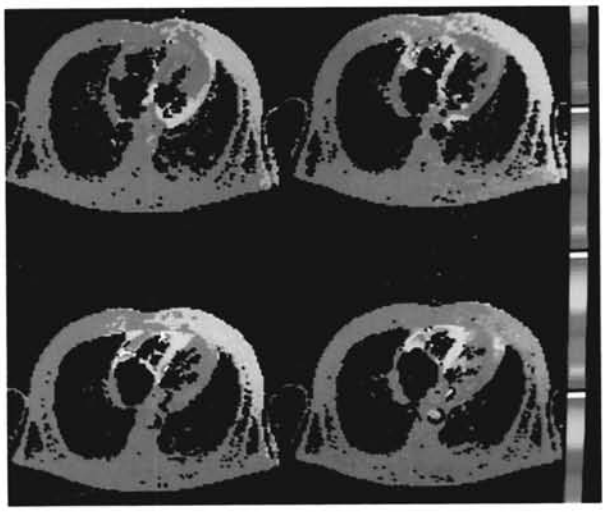

10

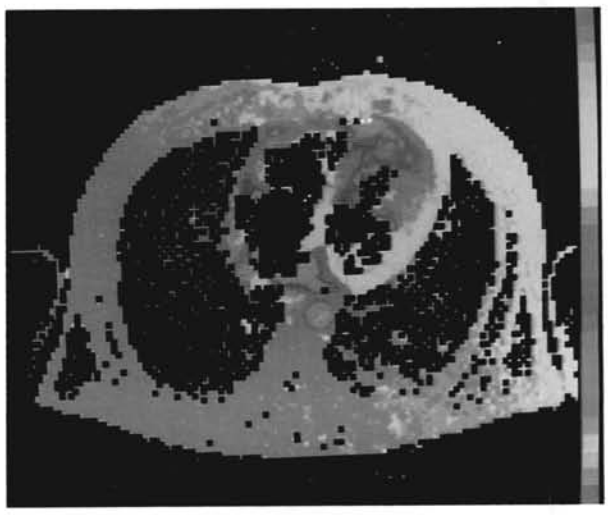

11

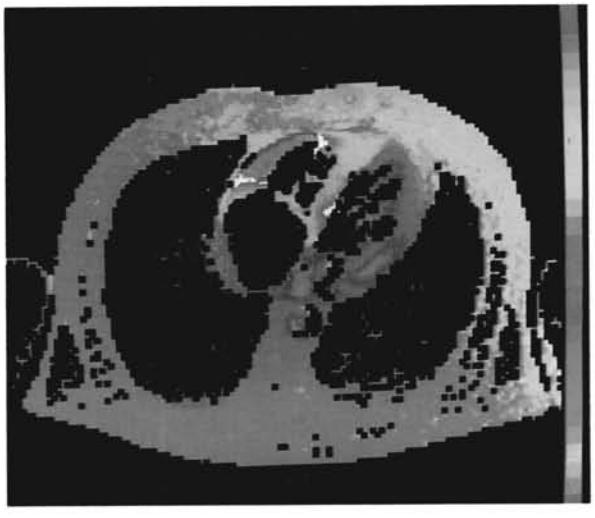

12

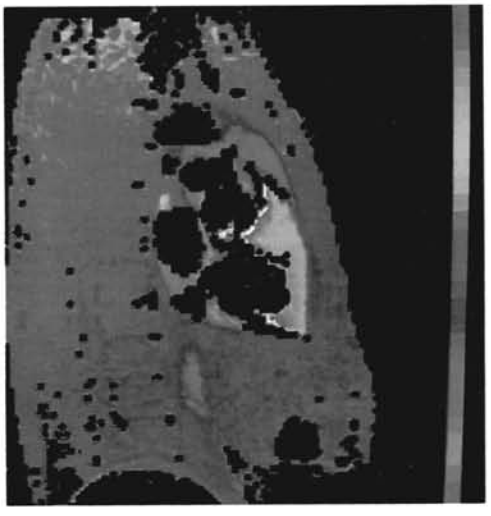

13

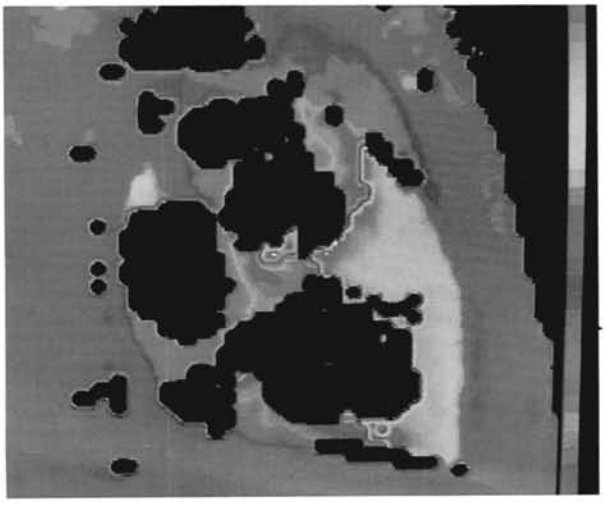

FIG. 9. Phase (velocity) images for the same scans as shown in Fig. 8. One color scale extends from −180° (bottom) to +180° (top). The stationary anatomy is displayed in green.

FIG. 10. Early systole velocity image. Flow speeds in the aorta can be calculated to range from 6 to 10 cm/s (blue and violet areas in the aorta, respectively).

FIG. 11. Midsystole velocity image. The blue region of the heart wall is moving fast to the right, giving a phase shift of approximately 270°. The papillary muscles, also in blue, extend to the left, giving a negative phase shift.

FIG. 12. Velocity image for the same slice as Fig. 14. The yellow region is moving fastest downward. The blue region under the heart represents flowing blood in the aorta.

FIG. 13. Zoomed image of Fig. 12 to show the heart only.

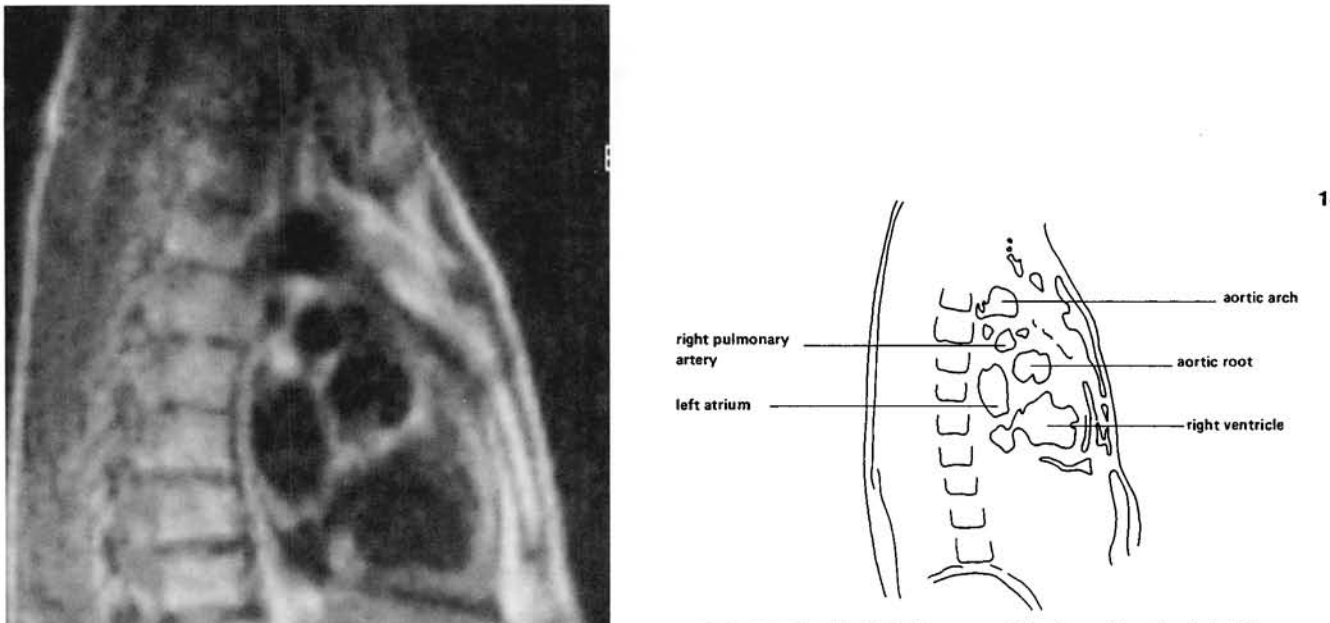

FIG. 14. Sagittal NMR scan of the heart in diastole **(a)** with anatomical details of this slice **(b).** (Reproduced with permission from S. Karger AG, Basel, ref. 1.)

Nuclear magnetic resonance imaging has the advantage of producing images in any slice orientation. This is demonstrated in Fig. 14a, which shows a midsagittal slice in the diastolic phase, in fact the rapid filling phase of the heart cycle, 480 ms after the R-wave. Some anatomical details are shown in Fig. 14b. The corresponding velocity image is shown in Fig. 12 where the measuring gradient direction is from bottom to top. Green is again the color for stationary spins in this image without gradient misadjustment artifact. The blue part under the heart represents downward flowing blood in the aorta. Assuming downward motion in this phase of the heart cycle, the yellow region is moving fastest, sliding against the stationary sternum. The same image can be zoomed in to show the heart only (Fig. 13). The white 180° part is interpolated to be a blue-yellow transition in this process.

DISCUSSION

An important NMR application can be the imaging of vessels as in digital subtraction angiography. The motion of blood makes the vessels contrast with the surrounding tissue. By ECG synchronized NMR imaging of a thick slice containing the vessels of interest, a projection imaginary image can be made, showing the vessels only. Different speeds in one gradient direction, e.g., due to vessel orientation, will give different intensities for each vessel. This gives better discrimination of overlapping vessels, a problem often encountered in vascular imaging.

These results indicate only some of the possibilities of ECG synchronized NMR velocity imaging. A wide range of applications can be thought of which include all parts of the body with heart induced motion, such as detection of impaired motion of heart walls, quantitation of heart wall velocities, blood flow velocity and volume flow quantitation, detection of obstructions in vessels, and comparison of left and right side blood flow.

Finally, the described method can be extended to three-dimensional Fourier transform imaging to obtain anatomical and velocity images of contiguous slices in the same heart phase.

Acknowledgment: The author wishes to thank Dr. C. M. J. van Uijen of Philips Research Laboratories for his valuable comments and Ms. Ingrid Schmitz for the accurate preparation of the manuscript.

REFERENCES

1. van Dijk P. ECG-triggered NMR imaging of the heart. *Diagn Imaging* 1984;53:29–37.
2. Hawkes RC, Holland GN, Moore WS, Roebuck EJ, Worthington BS. Nuclear magnetic resonance (NMR) tomography of the normal heart. *J Comput Assist Tomogr* 1981;5:605–12.
3. Alfidi RJ, Haaga JR, El Yousef SJ, et al. Preliminary experimental results in humans and animals with a superconducting, whole-body, nuclear magnetic resonance scanner. *Radiology* 1982;143:175–81.
4. Heneghan MA, Biancaniello TM, Heidelberger E, Peterson SB, Marsh MJ, Lauterbur PC. Nuclear magnetic resonance zeugmatographic imaging of the heart: application to the study of ventricular septal defect. *Radiology* 1982;143: 183–6.
5. Herfkens RJ, Higgins CB, Hricak H. Nuclear magnetic resonance imaging of the cardiovascular system: normal and pathologic findings. *Radiology* 1983;147:749–59.
6. Williams ES, Kaplan JI, Thatcher F, Zimmerman G, Knoebel SB. Prolongation of proton spin lattice relaxation times in regionally ischemic tissue from dog hearts. *J Nucl Med* 1980;21:449–53.
7. Brady TJ, Goldman MR, Pykett IL, et al. Proton nuclear magnetic resonance imaging of regionally ischemic canine hearts: effect of paramagnetic proton signal enhancement. *Radiology* 1982;144:343–7.
8. Herfkens RJ, Sievers R, Kaufman L, et al. Nuclear magnetic resonance imaging of the infarcted muscle: a rat model. *Radiology* 1983;147:761–4.
9. Higgins CB, Herfkens RJ, Lipton MJ, et al. Nuclear magnetic resonance imaging of acute myocardial infarction in dogs: alterations in magnetic relaxation times. *Am J Cardiol* 1983;52:184–8.
10. Moran PR. A flow velocity zeugmatographic interlace for NMR imaging in humans. *Magn Res Imaging* 1983;1:197–203.
11. Singer JR. NMR diffusion and flow measurements and an introduction to spin phase graphing. *J Phys* [*E*] 1978;11: 281–91.
12. Kaufman L, Crooks LE, Sheldon P, Hricak H, Herfkens RJ, Bank W. The potential impact of nuclear magnetic resonance imaging on cardiovascular diagnosis. *Circulation* 1983; 67:251–7.